

News from the Experiments

IceCube-Gen2

Albrecht Karle reports:

The IceCube-Gen2 collaboration has successfully concluded a significant milestone: the completion of a comprehensive Technical Design Report [1]. This 370-page document, divided into three parts, serves as a testament to their collective efforts and dedication.

- Part I, Science and Conceptual Design is primarily an update of an earlier whitepaper.
- Part II, Detector and Performance, documents the 3 major detector components (optical, radio, surface array) plus data acquisition & data handling.
- Part III, Detector Construction and Logistical Support Requirements provides an in-depth view of the construction and logistics.

The document was released at a time when questions were raised about the supportability of IceCube-Gen2.

As reported earlier, the Astro 2020 Decadal review and, most recently, the P5 report strongly endorse IceCube-Gen2. The follow-ups of NSF's two flagship astrophysics and cosmology programs at the South Pole, IceCube-Gen2 and CMBS4, were among the top five large projects.

However, NSF's Antarctic Program is focused on infrastructure modernization, which has fallen behind in the last decade. At the recent High Energy Physics and Astrophysics Panel (HEPAP) meeting, NSF announced that CMBS4, the highest-ranked project, could not go ahead at the South Pole as planned. NSF emphasized the need to refurbish the station

infrastructure. NSF Physics director, Saul Gonzales, pointed out that they *"are focused on completing the ongoing IceCube Upgrade. Results from that Upgrade will inform future plans of IceCube-Gen2"*. Thus, NSF has made it clear that the IceCube Upgrade is a priority. While infrastructure modernization provides important constraints, the scientific opportunities are also very clear to them; see the conclusion from Dr. Gonzales. *"There is a shift in the center of gravity of the field from collider techniques to cosmo/astro techniques. We heard that message and are thinking about how to follow that shift to these scientific opportunities."*

The Project team points out that it takes two to three years after the project starts until construction at the South Pole go into high gear (see schedule in the TDR) and that there are ways to mitigate some of the issues. People who have experience with IceCube as well as South Pole Telescope, point to the fact that those detectors were built simultaneously with each other and the South Pole station. If interested to read more, see a recent article in the Symmetry magazine on the discussion [2]. The IceCube and the CMB community believe the problem is not fundamental. After considering the planned infrastructure efforts, IceCube is looking for a project to start by 2029.

[1] <https://icecube-gen2.wisc.edu/science/publications/tdr/>

[2] https://www.symmetrismagazine.org/article/a-harsh-environment-for-life-an-ideal-environment-for-research?language_content_entity=und

KM3NeT: ORCA sea operation

Paschal Coyle reports:

During a short marine operation, 2-4 June 2024, four new detection units were added to KM3NeT/ORCA. A fifth detection unit was also connected, but tests prior to unfurling indicated some issues, so it was recovered. An autonomous acoustic beacon was also recovered for refurbishment. These beacons are used by the acoustic positioning system to continuously measure the real-time positions of the optical modules to about 10 cm precision. ORCA now comprises 23 deployed detection units. A special shout out to Evelyne Garcon and Marie-Ange Cordier who contribute to the final steps of the detection unit integration at CPPM and play a key role in the deployment on the boat.

Video:

https://youtu.be/BJKDEJ6Hb4o?si=n116SE6mq_gHLRvD



The deck of Castor-2 of Foselev Marine loaded with the new detection units awaiting deployment, at dawn while starting up the campaign.

KM3NeT: Collaboration meeting

From June 10-14, The Royal Netherlands Institute for Sea Research, NIOZ, in Texel (Netherlands) hosted the summer meeting of KM3NeT. MPI for Radio Astronomy (Bonn) and Khalifa (University Abu Dhabi/ UAE) have been accepted as full members.



A DU starting its journey to the bottom of the sea.



Into the blue!

Baikal-GVD

On June 4-7, JINR Dubna hosted the spring meeting of the Baikal collaboration, with about 40 face-to-face and 10-15 on-line participants. Apart from members of the collaboration itself, Mingjun Chen from IHEP Beijing and three colleagues from the MEPhi NEVOD group were participating. The Baikal collaboration is considering to perform a precise measurement of their OM angular sensitivity in the huge NEVOD water tank in Moscow which is equipped with optical quasi-spherical modules and surrounded by several types of tracking detectors. The corresponding plans were presented in one of the talks. The practical experience with connecting and deploying the Chinese string with its 20" OMs and the first results from the data evaluation were reported in two talks, one by Bair Shaibonov (JINR) and one by Mingjun Chen.



In 2025, it is planned to install two clusters (18 strings in total), one or two strings of a fiber-optic cluster and a full-scale string with 24 Chinese-made optical modules.

P-ONE

On May 13-17, the Erlangen Centre for Astroparticle Physics (ECAP) hosted a collaboration meeting of the P-ONE project. Physicists, oceanography experts, project managers, and engineers met to discuss and plan the next crucial steps of the project: the first string to be built, the next few strings after that, and finally the plans for the full detector of 70 strings. The meeting was hosted in the recently built "ECAP

Laboratory" building, where close to 50 participants (see the picture) could easily be accommodated.



In addition to a fruitful scientific meeting, participants explored Erlangen and participated in various activities outside the meeting. The local beer gardens & restaurants attracted many of them after the meeting days had concluded, peaking with the "Bergkirchweih" beer festival that started on May 16.

RNO-G

RNO-G has started its field season. At present, RNO-G has 7 operational stations, the current goal is 35 at the end of 2026. The drilling team at Summit Station has been putting together the newly upgraded drill and has started its endeavor of drilling holes for new RNO-G stations. As frequently in the early season, the team has been mostly battling bad weather which precludes travel off station and results in a lot of digging, see the figure below. The new automation of the drill has been working well during the first holes. But as everyone experienced with (Ant-)arctic experiments knows, the season will most likely have surprises in store. A full report will follow, once the season has been completed in August.



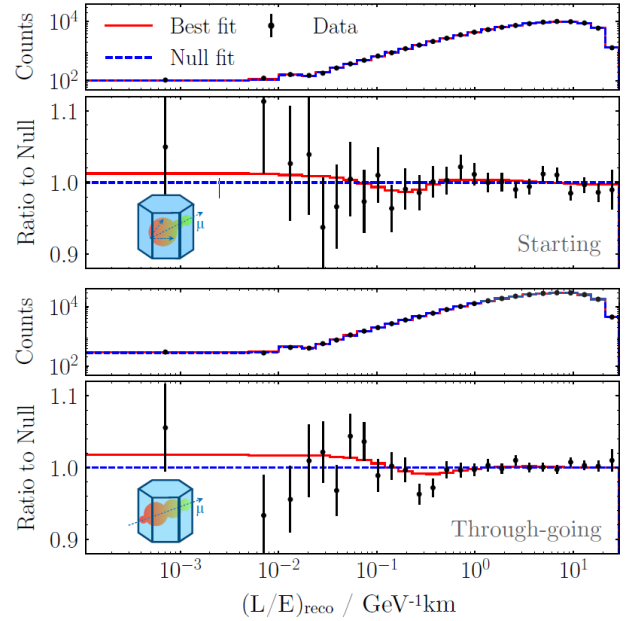
Publications

Sterile neutrino time for IceCube! Three recent papers address the search for eV-sterile neutrinos. Predicted propagation effects in matter enhance the signature of a sterile neutrino through a resonance as atmospheric neutrinos from the Northern Hemisphere traverse the Earth. The first paper presents a 3+1 sterile neutrino search using 10.7 years of IceCube data and muon neutrinos with energies ranging from 0.5 to 100 TeV. The second paper is a kind of technical addendum to the first one and gives a detailed description of the improvements in modeling neutrino flux and detector response which have led to the results presented in the first paper. The third paper uses 7.6 years of muon neutrino events in the energy range 0.5-10 TeV and fits not only two, but three parameters: the mass squared splitting between the heaviest and lightest mass state (Δm^2_{41}), the mixing matrix element connecting the fourth mass state to the muon flavor state ($|U_{\mu 4}|^2$), and to the tau flavor state ($|U_{\tau 4}|^2$), respectively.

The paper *A search for an eV-scale sterile neutrino using improved high-energy ν_μ event reconstruction in IceCube* is submitted to Phys. Rev. Letters and posted at [2405.08070 \(arxiv.org\)](https://arxiv.org/abs/2405.08070). The main contributions to the paper come from the IceCube groups at Harvard University, MIT, and University of Texas/Arlington.

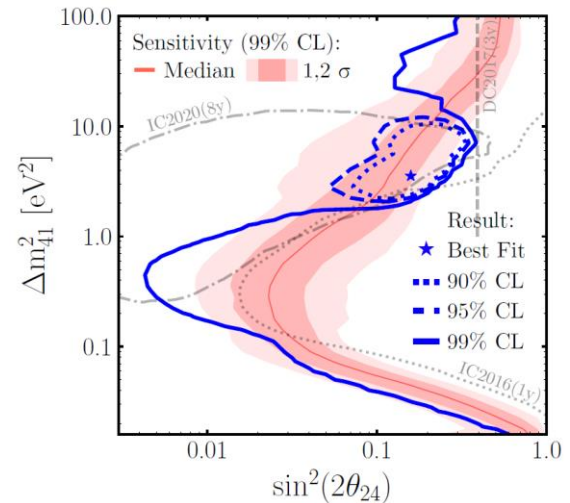
The corresponding paper from four years ago (2020) <https://arxiv.org/pdf/2005.12943> was based on ~300k through-going muon tracks from atmospheric neutrino interactions with energies 0.5 – 10 TeV. In the present paper, the energy range is extended to 100 TeV. Improved reconstruction methods and a BDT analysis (background reduced by a factor of 2, signal efficiency increased by a factor 2), plus improved flux estimates and a better detector description are applied, furthermore not only through-going tracks but also starting tracks events are included.

The reconstructed L/E distributions for the selected events (next figure) show a good agreement between data and the prediction at the best-fit point of the analysis for both through-going and starting tracks.



L/E distributions: Data points are black markers with error bars representing the Poissonian statistical error. The solid red and blue lines show the best-fit sterile neutrino hypothesis and the null (no sterile neutrino) hypothesis, respectively, with nuisance parameters set to their best-fit values in each case. The top (bottom) panels show the number of events and the ratio to the null hypothesis in each bin for starting (through-going) events.

Both a frequentist and a Bayesian approach have been performed. The results of the frequentist analysis are shown in the next figure, with a best-fit point at $\sin^2(2\theta_{24}) = 0.16$ and $\Delta m^2_{41} = 3.5 \text{ eV}^2$ (p-value 3.1%)



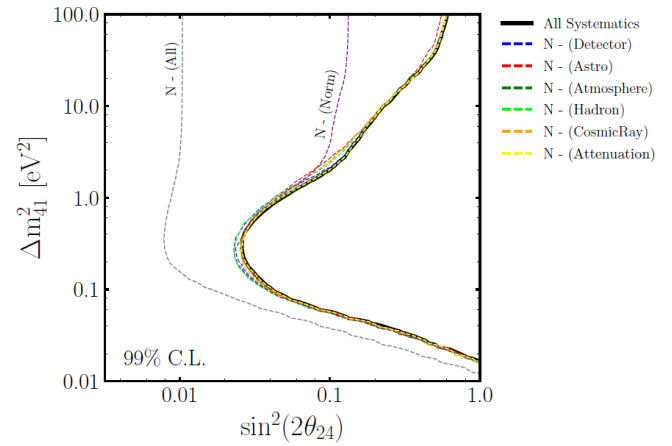
Frequentist analysis. The 90%, 95%, and 99% C.L. contours, assuming Wilks' theorem, are shown as dotted, dashed, and solid blue lines, respectively. The red bands show the region where 68% and 95% of the pseudo-experiment 99% C.L. observations lie; the red line corresponds to the median. Previous measurements from IceCube at 90% C.L. are shown in grey. The region right of the blue full line is excluded with 99%.

The second paper “*Methods and stability tests associated with the sterile neutrino search using improved high-energy ν_μ event reconstruction in IceCube*” has been submitted to Phys. Rev. D and posted at [2405.08077 \(arxiv.org\)](https://arxiv.org/abs/2405.08077). Again, the main contributions come from the IceCube groups at Harvard University, MIT, and University of Texas/Arlington.

The results of this and of the first paper are also presented at the IceCube webpage: <https://icecube.wisc.edu/news/research/2024/05/search-for-elusive-sterile-neutrino-continues-with-improved-high-energy-muon-neutrino-reconstruction-in-icecube/>

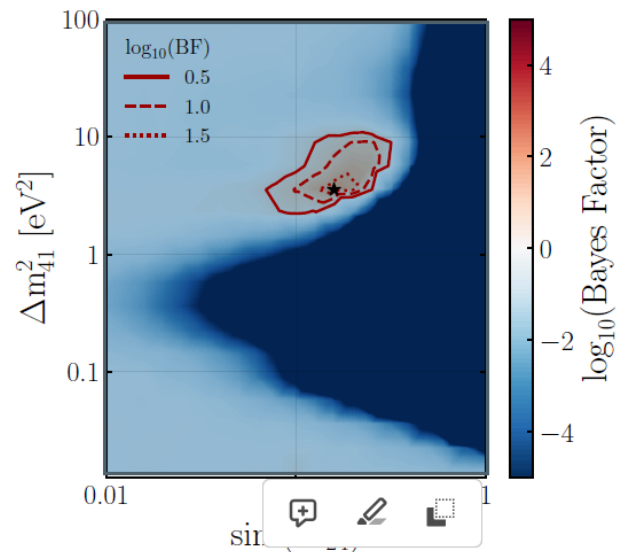
The article describes the improvements compared to past analyses, including the improved reconstruction and the study of sources of systematic uncertainty. It provides details of the fit quality and discusses stability tests for which the data have been split into separate sub-samples. The improvements include reconstruction algorithms (atmospheric muon background rejection, energy estimation, starting event classification, neutrino type classification), description of the conventional atmospheric neutrino flux and constraints to non-conventional flux, detector parameters (bulk ice, DOM response, ...), and neutrino attenuation for Earth passage.

The next figure quantifies the influence of each uncertainty source on the expected sensitivity for this analysis. Each curve represents a scenario where the nuisance parameters linked to one type of uncertainty are held constant at their central values while allowing others to fluctuate within their constraints. At large Δm_{41}^2 , the most significant impact stems from normalization, followed by astrophysical and cosmic-ray flux uncertainties. Conversely, at low Δm_{41}^2 , the dominant factors are uncertainties in the detector and hadronic yields. While removing most of the systematic uncertainties individually exhibits minimal impact on sensitivity, the collective effect of systematics is more substantial when all are removed simultaneously.



Effects of different systematic groups on the sensitivity. The analysis sensitivity at 99% C.L. is shown as a solid black line. The dashed lines show the estimated sensitivity when a given systematic uncertainty category is removed.

This paper also displays the Bayesian fit results (in addition to the frequentist results shown in the first paper):



Bayesian result. The color scale shows the \log_{10} of the BF relative to the null hypothesis. The dotted, dashed, and solid black contours correspond to $\log_{10}(BF)$ values 0.5, 1.0 and 1.5. The best model is marked with a black star. Systematic uncertainties are marginalized for each point in the scan.

After unblinding, an extended set of studies was performed where the data was split into separately fitted sub-samples. The paper has shown that the results are stable, including for the energy and zenith angle split cases. The reconstruction and stability test techniques reported in the present paper will also be applicable in future IceCube analyses.

The third paper *Exploration of mass splitting and muon/tau mixing parameters for an eV-scale sterile neutrino with IceCube* is posted at <https://arxiv.org/pdf/2406.00905> and has been submitted to Phys.Lett.B. Main contributions to this paper come from the groups at the Massachusetts Institute of Technology, the Harvard University, and the University of Delaware.

The paper presents the first three-parameter fit to a 3+1 sterile neutrino model using 7.634 years of data on muon-neutrino charged-current interactions in the energy range 0.5-10 TeV. The three parameters are the mass-squared splitting between the heaviest and lightest mass state (Δm_{41}^2), the mixing matrix element connecting muon flavor to the fourth mass state ($|U_{\mu 4}|^2$), and the element connecting tau flavor to the fourth mass state ($|U_{\tau 4}|^2$).

Here are the definitions (relations to mixing angles):

$$U_{3+1} = \begin{pmatrix} U_{e1} & U_{e2} & U_{e3} & U_{e4} \\ U_{\mu 1} & U_{\mu 2} & U_{\mu 3} & U_{\mu 4} \\ U_{\tau 1} & U_{\tau 2} & U_{\tau 3} & U_{\tau 4} \\ U_{s1} & U_{s2} & U_{s3} & U_{s4} \end{pmatrix}$$

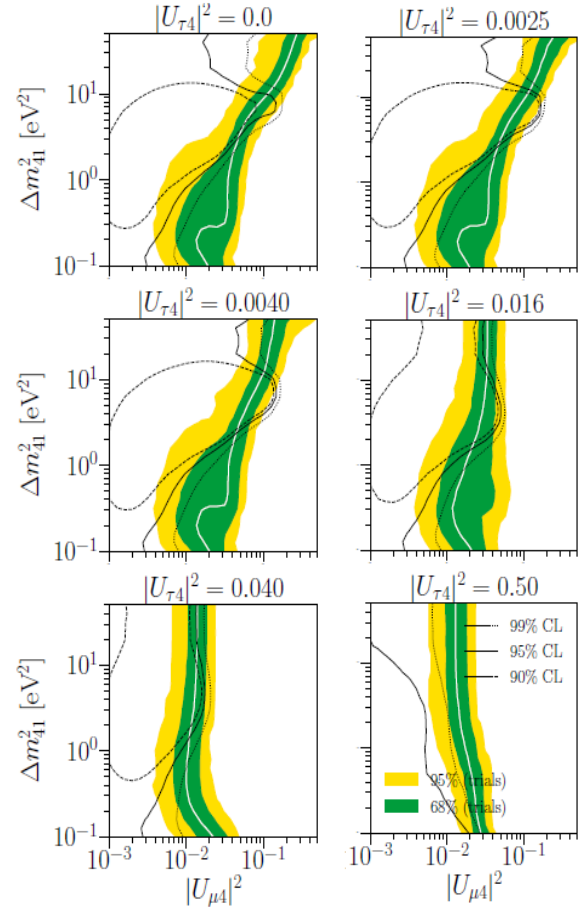
$$|U_{\mu 4}|^2 = \sin^2 \theta_{24}$$

$$|U_{\tau 4}|^2 = \sin^2 \theta_{34} \cos^2 \theta_{24}.$$

The result is consistent with the no-sterile neutrino hypothesis with a probability of 4.3%.

Profiling the likelihood of each parameter yields the 90% confidence levels: $2.4 \text{ eV}^2 < \Delta m_{41}^2 < 9.6 \text{ eV}^2$, $0.0081 < |U_{\mu 4}|^2 < 0.10$ and $|U_{\tau 4}|^2 < 0.035$, which narrows the allowed parameter-space for $|U_{\tau 4}|^2$. The primary result of this analysis is the first map of the 3+1 parameter space exploring the interdependence of Δm_{41}^2 , $|U_{\mu 4}|^2$, and $|U_{\tau 4}|^2$.

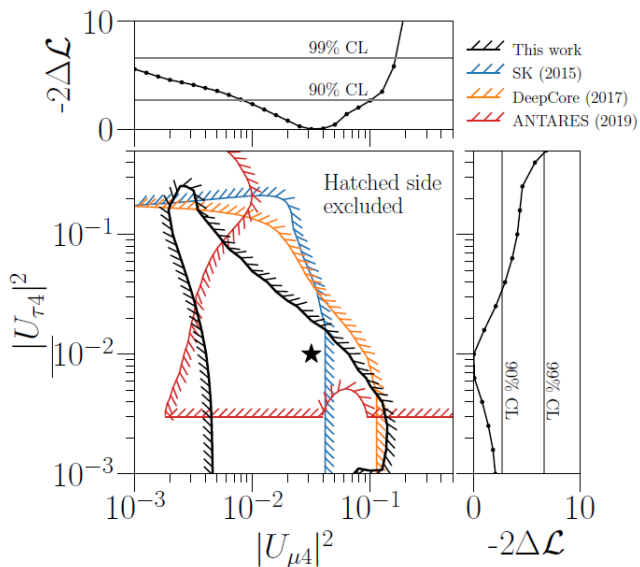
The best-fit point is found at $\Delta m_{41}^2 = 5.0 \text{ eV}^2$, $|U_{\mu 4}|^2 = 0.032$, and $|U_{\tau 4}|^2 = 0.010$. The 99%, 95%, and 90% confidence levels (CL) of the fit are shown in the next figure, assuming Wilks' theorem and three degrees of freedom for a subset of the $|U_{\tau 4}|^2$ range sampled (see the paper for details). The figure demonstrates the strong influence which the $|U_{\tau 4}|^2$ parameter has for the allowed regions in Δm_{41}^2 and $|U_{\mu 4}|^2 = \sin^2 \theta_{24}$.



The 99%, 95%, and 90% CL regions for a selection of $|U_{\tau 4}|^2$ values tested. The contours are drawn assuming Wilks' theorem with 3 degrees of freedom (see for details the paper). The colored bands show where the middle 68.27% (green) and 95.45% (yellow) of simulated 99% CLs for no signal lie.

As seen in the figure next page, part of the IceCube allowed region (not the best fit!) is compatible with limits from other experiments when the analysis is reduced to two parameters, $|U_{\mu 4}|^2$ and $|U_{\tau 4}|^2$, through profiling in order to enable comparison. Note that information is lost when one reduces to these parameters because the full 3+1 model predicts dependence on Δm_{41}^2 in the range of 1 to 10 eV^2 , as can be seen in the three parameter fits presented in figure above. Hence, experiments that by design average over this range of Δm_{41}^2 lack essential sensitivity.

The results of this paper, therefore, illustrate the importance of expanding to three-parameter fits for Δm_{41}^2 , $|U_{\mu 4}|^2$, and $|U_{\tau 4}|^2$ to test the 3+1 model.



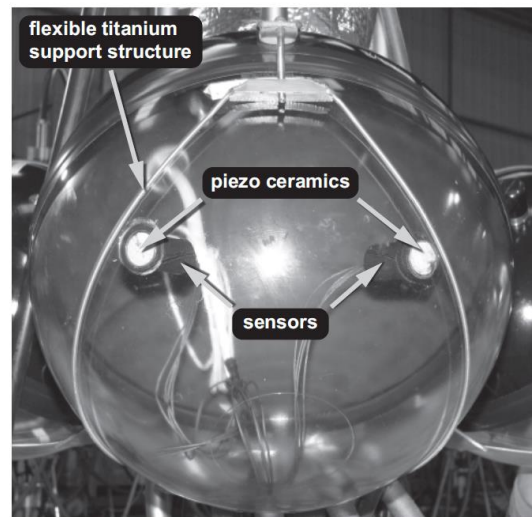
Comparison of the 90% CL contour of this analysis to Super-Kamiokande, DeepCore, and ANTARES. Since other experiments do not perform a 3D fit over $(\Delta m^2_{41}, |U_{\mu 4}|^2, |U_{\tau 4}|^2)$, results are profiled over Δm^2_{41} to allow the comparison (bottom left). The hatched lines indicate the area which is excluded by the respective experiment. For ANTARES, the horizontal line at $|U_{\tau 4}|^2 = 0.003$ indicates the lower bound of that analysis. The top and right plots show the test statistic distribution when all parameters but $|U_{\mu 4}|^2$ ($|U_{\tau 4}|^2$) have been profiled over. The relatively shallow $-2\Delta \log L$ distributions indicate the best fit point (star) is not strongly favored within the wide allowed range. The two gray lines mark the 90% and 99% critical values for Wilks' theorem in one dimension.

The [ANTARES collaboration](#) has posted a paper *Acoustic Positioning for Deep Sea Neutrino Telescopes with a System of Piezo Sensors Integrated into Glass Spheres* at [2405.07230 \(arxiv.org\)](https://arxiv.org/abs/2405.07230) (submitted to Experimental Astronomy). The corresponding author is Robert Lahmann (ECAP Erlangen).

For acoustic position calibration, KM3NeT employs piezo ceramics glued to the inside of the DOMs as receivers, rather than hydrophones that are exposed to the ambient pressure. Aim of the paper is the investigation of the acoustic properties of the combined system of piezo sensor and glass sphere, as the assumption made for position reconstruction – the signals travelling the complete distance from the emitter to the receiver in water – cannot be exactly true.

The acoustic test system AMADEUS of ANTARES contained a storey with three “acoustic modules” in

which piezo sensors were glued to the inside of – otherwise empty – glass spheres that are identical to those used in KM3NeT, see figure. These acoustic modules are ideally suited to investigate the propagation of sound from the sea water to the piezo sensors on the inside of the glass spheres.

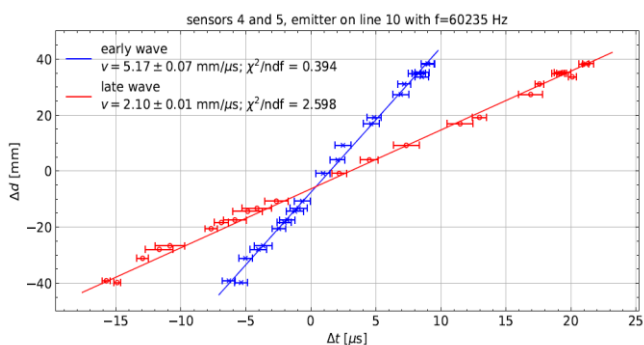


Top: ANTARES storey with acoustic modules during deployment; Bottom: acoustic module.

The acoustic emitters of ANTARES, installed on the sea floor, emitted signals with frequencies from 46545 to 60235 Hz. For a given acoustic module, differences in distance Δd travelled by the signal from an acoustic emitter to the two piezo sensors could be calculated. These could then be related to the difference Δt in

time of arrival of the signal at the two sensors. Two waves propagating through the glass sphere are found resulting from the excitation by the waves in the water. These can be qualitatively associated with symmetric and asymmetric Lamb-like guided waves* of zeroth order: a fast (early) one with $v_e \approx 5\text{mm}/\mu\text{s}$ and a slow (late) one with $v_l \approx 2\text{mm}/\mu\text{s}$. (*Lamb waves are superpositions of longitudinal and transverse waves, propagating one-dimensionally in a solid plate of given thickness, satisfying the boundary conditions for an idealized experimental setup).

for which the effect is expected to be smaller, though, as the piezo sensor is located close to the lowest point of a DOM, resulting in shorter distances propagated in the glass sphere by signals from acoustic emitters on the sea floor.



Speed of sound derived from a linear fit for the early and late wave for signals from one of the ANTARES emitters. For each run, the average orientation of the storey was determined, which corresponds to a particular value of Δd on the y-axis. Each run contributes a value for Δt_e and Δt_l , for the early and late wave, respectively.

The late wave is dominant with an amplitude $\gtrsim 10$ times higher than that of the early wave. The measured phase velocities of the two waves agree with the phase velocities of Lamb waves – calculated for a flat plate with finite thickness and infinite extend in the other two dimensions – on a level of 10% for the zeroth symmetric and asymmetric mode for the range of frequencies of the ANTARES acoustic emitters and the thickness of the glass sphere. The speed of sound in water at the depth of the acoustic modules is $v_{\text{water}} = 1.54\text{ mm}/\mu\text{s}$. The notion of the faster wave propagating through the glass and the slower one through the water, exciting the glass sphere “along the way” is not supported by the observations.

Taking the findings of the paper into account improves the accuracy of the position calibration with AMADEUS. The results can be transferred to KM3NeT,

Impressum
 GNN Monthly is the Monthly Newsletter of the Global Neutrino Network
<https://www.globalneutrino.org>
 Editor: Christian Spiering, for the GNN Board
christian.spiering@desy.de